Unsteady State Mass Transfer from Gas Bubbles—Liquid Phase Resistance

PANG-SHENG LI, FRANK B. WEST, WILLIAM H. VANCE, and RALPH W. MOULTON

University of Washington, Seattle, Washington

Liquid phase mass transfer coefficients were determined for streams of bubbles of pure oxygen, 10% carbon dioxide in air, and 10% chlorine in air all rising in water. The results were compared with coefficients predicted by Higbie's equation for unsteady state diffusion into transient films. The observed coefficients for oxygen and carbon dioxide were slightly higher than predicted. The experimental absorption coefficients based on the free chlorine concentrations were in good agreement with the predictions assuming simultaneous irreversible reaction with the transient water film and a pseudo first-order reaction rate constant of 13.7 sec.$^{-1}$.

The mechanism of mass transfer between gas bubbles and liquids has been investigated in detail only recently despite its importance in distillation and absorption operations. In general engineering practice, it is assumed that mass transfer from the interface between two fluids into either fluid phase can be correlated by equations of the type

$$\frac{dn}{dt} = k_L \, a(C_i - C_m) \tag{1}$$

When the fluid phases have internal motion, the coefficient has generally been considered to be equal to the diffusivity of the material being transferred divided by an effective film thickness. This concept corresponds to steady state diffusion across a stagnant film separating the interface from the bulk of the phase which is considered to be well mixed internally. To account for observed results, it has been necessary to allow the effective film thickness to vary with the diffusivity of the solute.

In 1935 Higbie (*15*) pointed out that in most commercial types of mass transfer equipment patches of interface are continually appearing and disappearing with lives of the order of only 0.01 to 0.10 sec. Under such conditions little solute should penetrate a stagnant surface film of any reasonable thickness, let alone come to steady state diffusion across it. Higbie suggested that each new patch of film might be considered to be stagnant and infinite in thickness over the brief period of its life t_e. Such patches have since been called *transient films* to emphasize their transient nature (*27*). Assuming the solute concentration at the interface C_i to be constant over the life of the film, Higbie derived the following equation for a mass transfer coefficient to fit the k_L of Equation (1):

$$k_L = 2\sqrt{\frac{D}{\pi t_e}} \tag{2}$$

A patch of interface has the same life for the transient films on either side of it. By Equation (2) the ratio of the k's for a solute in the two phases would be the square root of the ratio of its diffusivities in the two phases. Hence the ratio of k's for a solute will be constant if Equation (2) holds. For a constant ratio of k's and for equilibrium at the interface, C_i should be constant over the life of the films as assumed in the derivation. Accordingly, these individual k's calculated from Equation (2) can be combined into overall coefficients in the usual manner. Danckwerts (*5, 6, 7*) has derived similar equations for cases involving interfacial resistances, chemical reactions, and variable life expectancies for various patches of interface. It has been well established that internal circulation often does exist in bubbles and drops as called for in these equations (*10, 16, 20*).

To apply Higbie's equation it is only necessary to have the diffusivities of the solute and to estimate t_e. For gas bubbles in liquids Higbie suggested that t_e might be roughly approximated as the time for the bubbles to rise through a horizontal plane, that is, through a distance equal to their vertical diameters. It has been objected (*11*) that this is far too rough an approximation, that a patch of interface passing down over the surface of a spherical bubble would have to be joined by new patches with shorter lives in order to cover the expanding profile of the bubble. This objection may be valid but is not necessarily so. Each patch of interface can be considered to be a zone or ringlike element which expands in circumference and contracts in width so as to keep its area and surface free energy constant as it passes down over the bubble. The area of such an element on a spherical bubble of radius r_s is given by the equation

$$da = 2\pi r_s^2 \sin\alpha \; d\alpha = 2\pi r_s \; dh \tag{3}$$

As indicated by the equation, da remains constant as the element passes over the bubble, provided that dh remains constant. For dh to remain constant, the vertical component of the interfacial velocity dh/dt must remain constant so that successive elements all descend the same vertical distance in the same period of time regardless of their location on the sphere. If dh/dt is constant at the velocity of rise of the bubble, then t_e would be the time for the sphere to rise through a distance equal to its own diameter. The required interfacial velocity would be V_t over $\sin\alpha$. It would vary from V_t at the equator to infinity (for an infinitesimal distance) at the poles with an overall average of $\pi V_t/2$. For spheroidal bubbles, the required relations would be somewhat more complex. These condi-

---

Pang-Sheng Li is at the College of Chemical Engineering, Shanghai, China; Frank B. West is with Shell Development Company, Emeryville, California; William H. Vance is with Bettis Atomic Power Laboratory, Pittsburgh, Pennsylvania.

tions are unlikely to be met precisely, but they may be met closely enough for Higbie's suggestion to be a close approximation to reality.

In 1946, Geddes (*12*) published a plate efficiency correlation in which Higbie's equation was used for predicting mass transfer coefficients for the liquid phase. In 1952, West, Gilbert, and Shimizu (*29*) published a second plate-efficiency correlation in which Higbie's equation was used for predicting the coefficients for both phases. (Observed efficiencies for either liquid or gas phase controlling corresponded to practically the same effective bubble sizes despite a 10,000 fold variation between liquid- and gas-phase diffusivities.) Higbie's equation has also been applied in various liquid-liquid extraction studies (*4, 11, 27, 28*).

In 1954, Hammerton and Garner (*13*) showed that Higbie's equation holds fairly well for the liquid phase around individual bubbles of ethane, ethylene, oxygen, carbon dioxide, and hydrogen rising through water provided that the bubbles were clean and larger than 0.033 milliliters in volume. Below this size, and for grease-contaminated bubbles, internal circulation was developed only partially if at all, and mass transfer rates were much lower than predicted. The bubbles formed in most commercial equipment are well above this size.

This paper gives the results of an independent check on the validity of Higbie's equation for the liquid phase in absorption from streams of gas bubbles by water (*18*). Results were obtained for pure oxygen, for 10% carbon dioxide in air, and for 10% chlorine in air. The experimental technique was quite different from that of Hammerton and Garner, and in the case of chlorine the solute reacts with the solvent. Allowance has been made in the computations for distortion of the bubbles.

EXPERIMENTAL

The experimental equipment (Figure 1) consisted of two absorption columns provided with a series of bubbling nozzles and with facilities for humidifying and metering the feed gas streams. Degree of absorption was determined chemically, bubble rates were determined stroboscopically, and rates of rise and bubble distortions were measured photographically.

The absorption runs were carried out in a 44-mm. diameter vertical glass column 55 cm. tall. A flat glass window was attached to the outside with the intervening space being filled with water to permit photographing the bubbles with a minimum of distortion. A meter stick at the front of the column was photographed along with the bubbles. This scale was calibrated for parallax by photographing a second meter stick inserted into the center of the water-filled column. The runs were carried out batch-by-batch, so a duplicate column was provided for adjusting gas and bubble rates before each run.

Rubber stoppers closing the bottom of each column contain flush mounted drain tubes and duplicate bubbling nozzles. The nozzles were made from straight-bore Pyrex glass tubing without firepolishing. The inside diameters determined by calibration with mercury are as follows:

Nozzle No.	21	31	22	32	41	51
I.D. cm.	0.0735	0.207	0.1064	0.290	0.456	0.620
Mounting	|←-Flush--→|		|←---Inverted *J* Tube---→|			

The first two nozzles were mounted with their tips flush with the upper surface of the stopper. It was necessary to insert glass wool into nozzle 31 up to within 3 mm. of the tip to prevent water from flowing back into the tube between bubbles. To avoid this difficulty the rest of the nozzles were bent in the form of an inverted letter *J* so that the bubbles were formed beneath the tips.

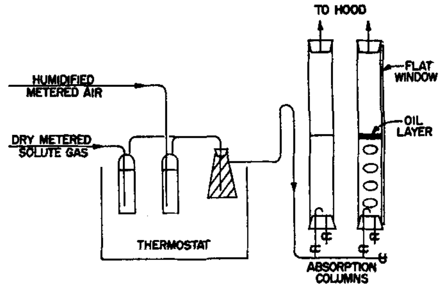

Fig. 1. Experimental absorption apparatus.

The solute gas streams were metered through carefully calibrated capillary orifices and were then saturated with water vapor to avoid cooling of the bubble interfaces by evaporation. Cylinder oxygen (99.5% pure) was supplied at constant pressure by means of a reducing valve. Carbon dioxide vapor (initially 98.5% pure) was drawn from the top of a cylinder of the liquid through two reducing valves in series with intermediate warming to avoid deposition of solid carbon dioxide in the second valve. A slight excess of chlorine vapor from the top of a liquid chlorine cylinder was brought to constant pressure in a barostat in which the excess chlorine escaped through an 8-mm. diameter leg immersed in zinc chloride solution. Air for diluting the carbon dioxide and chlorine was drawn from a constant pressure air line and was filtered through glass wool and water washed before being metered. Needle valves were used for regulating all streams except for the chlorine, where a screw clamp on a length of rubber tubing worked better. The metered streams passed through water saturators, the glass joints of which had been greased with Halocarbon stopcock grease. The humidified carbon dioxide and chlorine streams were diluted to 10% concentration with humidified air in a mixing chamber consisting of a flask filled with ¼-in. carbon Rashig rings. The chlorine flow meter was calibrated, and the carbon dioxide flow meter calibration was checked within 2% relative against the air flow meter by analysis of diluted gas streams with Hempel-buret and modified Gaillard bulb (9) procedures. For chlorine runs glass seals were substituted for flexible tube connections between the chlorine flow meter and the dilution flask.

The two columns, equipped with identical bubbling nozzles, were charged with distilled water to a depth of 30 cm. (or to 8 cm. for end effect runs). Humidified air was bubbled through the water to bring it to equilibrium with atmospheric oxygen and carbon dioxide partial pressures at test pressure and temperature. The temperature was held at 25°C. except for the first few oxygen runs. Ten ml. of paraffin oil were added to reduce end-effect mass transfer at the water surface. Feed gas was then bubbled into the duplicate column permitting the flow rates to be checked and adjusted under absorption conditions without contaminating the test column. When all was ready, the gas flow was suddenly diverted into the test column by simultaneously closing one pinch clamp and opening another. While absorption took place, the bubbling rate was determined by a type 631-B Strobotac which had been calibrated against an 1,800 rev./min. synchronous motor. Photographs were taken for each bubble size and bubbling rate and for most feed gas compositions. These permitted calculation of the apparent velocity of rise relative to the column walls from the ratio of the bubbles per second to the bubbles per centimeter height of column. The feed gas was shut off after 3 to 6 min. operation which was long enough to bring the water charge about half way to saturation in the oxygen and carbon dioxide runs. This minimized the effect of slight analytical errors on the amount of absorption without introducing appreciable error into the calculated driving force. The entire charge was then drained and analyzed.

After an oxygen absorption run the first few millimeters of the charge were discarded after all air was purged from the drain line. The remainder was collected beneath 15 ml. of paraffin oil in a 500 ml. weighed bottle (5 ml. of oil in a 125-ml. bottle for end-effect runs). After the sample was reweighed to determine the weight, the bottle was stoppered in such a way as to displace all air above the oil along with part of the oil layer. The contents were then analyzed by Winkler's method with 100% excess of potassium iodide. The overall accuracy of the sampling and analytical technique was checked by many dummy runs with air alone and with pure oxygen bubbling for 8 hr.

After the carbon dioxide absorption runs the charge was drained into excess barium hydroxide solution made from excess barium chloride and 0.1 N sodium hydroxide. After standing 10 min. in a stoppered bottle with occasional shaking, the mixture was backtitrated with standard hydrochloric acid to the phenophthalein end point. To minimize contamination from carbon dioxide in the surrounding air, the gas vented from the columns was discharged into a vacuum hood, and the analytical flask was swept with carbon dioxide-free air during the titration. The overall accuracy of the sampling and analytical technique was checked by dummy runs of 1-hr. duration with both the 10% feed and pure carbon dioxide.

In some of the chlorine runs the paraffin oil had been previously extracted with concentrated sulfuric acid and washed with caustic and water to remove any unsaturates. This treatment did not affect the results materially. Upon completion of the chlorine runs the charge was collected in about a 400% excess of potassium iodide solution. The iodine liberated was titrated with standard thiosulfate. Check determinations of the solubility of chlorine in water at partial pressures of 35 to 76 mm. Hg agreed with the data of Whitney and Vivian (*30*).

DISTORTION OF BUBBLES

The gas bubbles were quite noticeably distorted from the ideal spherical shape for all the sizes tested. This has two effects. It increases the interfacial area of the bubbles so that experimental coefficients based on the areas of spheres of the same volume would be somewhat high. Correcting for distortion lowers the experimental coefficients. A second effect is to shorten the axis of a bubble in the direction of motion so that predicted coefficients based on the diameters of spheres of the same volume would be too low. Correcting for distortion shortens t_e and increases the predicted coefficients. The overall effect of correcting for distortion is to decrease the observed coefficients and to increase the predicted coefficients, particularly for the larger bubble sizes where distortion is the greatest.

Experimental measurements of bubble distortion were confined to b/b_1, the ratio of the minor axis length to the major axis length. They were made for the oxygen bubbles only and included most but not all of the bubble sizes used. They were determined from high-speed flash pictures with a commercial strobo-light. Picture distortion was minimized by the short exposure (10^{-5} to 10^{-4} sec.) and by the flat window attached to the column.

The experimental data are indicated in Figure 2 in a plot of b/b_1 vs. r_s, the radius of a sphere of the same volume. Unfortunately, there was a great deal of variation in the ratios for each bubble size. Each point is an average of three to four measurements (representing the highest, lowest, and medium observed ratios where enough measurements were made). The variation may be due in part to tipping of the bubbles so as to enlarge the apparent minor axis and in part to actual oscillation around an equilibrium axis ratio. High-speed motion pictures might supply the complete answers. For the present it has been necessary to get along with the data of Figure 2 and to extrapolate these data to the smaller sizes which were not measured. A smoothed curve has been drawn through the data and extended to a ratio of unity at zero radius. The curve has been forced to approach unity asymptotically to agree with Van Krevelin's (*24*) observation that bubbles are not noticeably distorted in water below an r_s of 0.075 cm. Hughes and Gilliland (*16*) give a method for predicting b/b_1 for a bubble based on its terminal velocity of rise. The method depends on wind tunnel drag coefficients for solid oblate spheroids relative to those for solid spheres. The predicted ratios are 10 to 25% lower than the observed points in Figure 2.

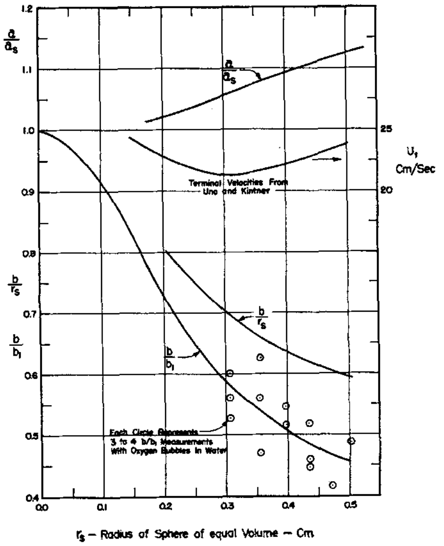

Fig. 2. Effect of size on bubble distortion and terminal velocities of rise.

In order to calculate correction factors for the distortion, it has been necessary to assume the bubbles to be oblate spheroids. The geometric relations used are as follows (*14*):

$$v = \frac{4}{3}\pi b_1^3\left(\frac{b}{b_1}\right) = \frac{4}{3}\pi r_s^3 \tag{3}$$

$$a = 2\pi b_1^2 + \pi\frac{b^2}{E}\ln\frac{1+E}{1-E} \tag{4}$$

where

$$E = \sqrt{1-(b/b_1)^2} \tag{5}$$

The correction factors calculated from these equations and the smoothed axis ratios are also plotted in Figure 2 as b/r_s and a/a_s. The spheroidal areas are 2 to 12% greater than the equivalent spherical areas, and the minor axes are 20 to 40% smaller than the equivalent spherical radii. No high accuracy can be claimed for these correction factors in view of the scattering of the data and of the approximation for the geometrical shape of the bubbles. They should at least be a great improvement over treating the bubbles as perfect spheres.

EXPERIMENTAL MASS TRANSFER COEFFICIENTS

The batch-by-batch nature of the absorption procedure simplified the procurement of precise experimental data but complicated their interpretation. It was necessary to derive (*18*) several special equations relating the mass transfer coefficient k_L to the amount of solute transferred. The derivations are outlined here in abbreviated form owing to their length and limited interest beyond this particular application.

The derivations begin with Equation (1) written for a single bubble of area a, risng through a batch of water of volume V_s for end-effect runs or V_t for normal runs. C_i is replaced by the equilibrium solubility C^*, since the predicted mass transfer resistance of the gas phase is zero for pure oxygen and only 1 to 2% of the total resistance with the other feed streams. For any given bubble, the bulk concentration of solute in the liquid phase C_m is assumed to be uniform throughout the column. While not strictly correct, this is a reasonable simplifying assumption based on mixing of the liquid by convection currents induced by the drag of the central stream of gas bubbles. The upward velocity of the central aerated core of liquid appears to be of the order of 5 to 10 cm./sec. based on the difference in velocities of rise between slowly formed bubbles and those studied here. This would give quite rapid circulation for runs of 3- to 6-min. duration.

Oxygen Absorption

For a slightly soluble pure gas like oxygen, C^* is equal to the initial value of C_o for all bubbles during a run and is substantially independent of the height of rise. The slight variation in partial pressure with static head is neglected. Changes due to desorption of nitrogen from the air-saturated water would be negligible even if all the dissolved nitrogen were desorbed. Accordingly, Equation (1) can be integrated for any single bubble rising through V_s or V_t in time t_s or t_t to give

$$n_t = k_{Lt}\, a(C_o^* - C_{mt})\, t_t \tag{6}$$

or

$$n_s = k_{Ls}\, a(C_o^* - C_{ms})\, t_s \tag{7}$$

Differential material balances relate n, N (the bubble rate) and $d\theta$ (an increment of time during the run) to V and dC_m. This permits substitution for the n's in the above equations and integration over the time interval θ_f. When one assumes that end effects are the same for the two columns, the mass transfer coefficient corrected for end effects will be given by

$$k_L\, \Delta t_{t-s} = k_{Lt}\, t_t - k_{Ls}\, t_s \tag{8}$$

Substituting the k_L t's from the integrals into Equation (8) one obtains the final relation:

$$k_L\, \Delta t_{t-s} = \frac{V_t}{aN\theta_f} \ln \left(\frac{C_o^* - C_{mo}}{C_o^* - C_{mf}} \right)_t - \frac{V_s}{aN\theta_f} \ln \left(\frac{C_o^* - C_{mo}}{C_o^* - C_{mf}} \right)_s \tag{9}$$

Experimental k_L values for oxygen absorption were calculated from Equation (9) for ten consecutive pairs of tall and short column runs covering seven different bubble volumes. Δt_{t-s}, the time for the bubbles to rise through V_t less that through V_s, was calculated from the two liquid depths and the observed velocity of rise relative to the column walls. C_o^* values were computed from the Henry's law constants (*17*) and the barometric pressure less the vapor pressure of water. The initial oxygen concentration for the air-saturated water was taken to be 0.21 C_o^*. The k_L's for the few runs not made at 25°C. were corrected to 25°C. by the assumption that k_L varies as the square root of the diffusivity.

Carbon Dioxide Absorption

For an impure solute gas such as carbon dioxide in air, the solute partial pressure varies with the amount of absorption from the bubble. C^* therefore varies with both the height of rise and with the elapsed time during the run. It can be related to dn for a bubble of volume v by the expression

$$dn = \frac{vm}{RT}\, dC^* \tag{10}$$

For the present case with only 10% solute in the gas, the bubble volume can be considered to be constant during its rise due to expansion under reduced static head largely offsetting absorption. Combining Equations (1) and (10) and integrating at constant C_m over the times for a bubble to rise through V_s and through V_t one gets two integrals which can be combined into

$$\Delta N_{OL} = N_{OLt} - N_{OLs} = \frac{aRT}{vm}\, (k_L\, \Delta t_{t-s}) \tag{11}$$

where

$$N_{OL} = \ln \frac{C_o^* - C_m}{C_p^* - C_m} \tag{12}$$

C_p^* corresponds to the residual partial pressure of solute gas at the top of the column at time θ during the run. It changes with time but can be related to dC_m by the differential material balance:

$$V\, dC_m = \frac{Nvm(C_o^* - C_p^*)\, d\theta}{RT} \tag{13}$$

Substituting C_p^* from Equation (12) into Equation (13) and integrating one obtains

$$\int_0^{C_{mf}} \frac{dC_m}{(C_o^* - C_m)(1 - e^{-N_{OL}})} = \int_0^{\theta_f} \frac{Nvm\, d\theta}{VRT} \tag{14}$$

or

$$e^{-N_{OL}} - 1 = \frac{VRT}{Nvm\,\theta_f} \ln \frac{(1 = C_{mf})}{C_o^*} \tag{15}$$

Equation (15) was used for computing the carbon dioxide N_{OL} values in order to calculate k_L from Equation (11). C_o^* was estimated from the Henry's law constant (*17*) and the inlet partial pressure computed as though the inlet gas were at barometric pressure. For each bubble size, three to twelve tall column runs and two to six short column runs were made and averaged to give more reliable data for use in the equation.

Chlorine Absorption

Chlorine absorption is complicated by a rapid but by no means instantaneous reaction of free or molecular chlorine with the solvent water. For adsorption of chlorine into water in a packed column, Vivian and Whitney (*26*) obtained results intermediate between those predicted for instantaneous chemical equilibrium throughout the solvent film with simultaneous diffusion of both free and combined chlorine, and negligible chemical reaction in the solvent film with diffusion of free chlorine only through the film followed by establishment of chemical equilibrium in the bulk of the water phase.

If instantaneous chemical equilibrium between free and combined chlorine is assumed for all parts of the liquid in the present batch-by-batch absorption runs, then k_L can be found from Equations (11) and (15) from total chlorine concentrations in the same manner as for carbon dioxide. The only complication is that m, the slope of the total solubility curve, varies with concentration (*26*). Fortunately, there is not much variation in slope over the

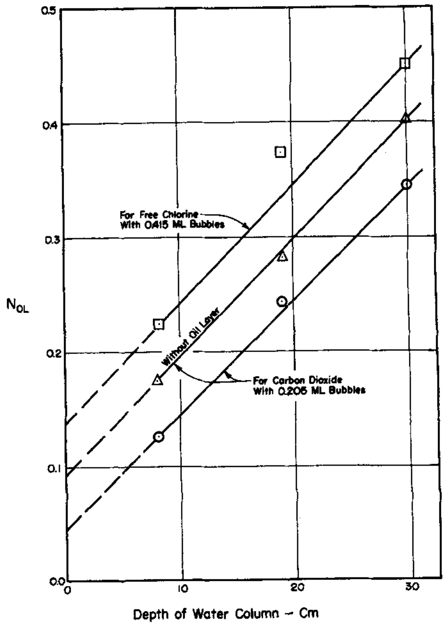

Fig. 3. End effects in absorption of carbon dioxide and of chlorine from air into water at 25°C.

range of interest permitting an average value of 6.47 × 10^6 mm. Hg/(g.-mole chlorine/ml. water) to be used at 25°C.

If negligible reaction is assumed to occur within the transient films, the total chlorine concentrations in the right-hand terms of Equations (12) and (13) should be replaced by the corresponding free chlorine concentrations. Similarly, m should be replaced by m_u, the slope of the free chlorine solubility curve which has a constant value of 12.15 × 10^6 mm. Hg/(g.-mole/ml. at 25°C) (*26*). These substitutions lead to integrals analogous to Equation (14), except that $C_o^* - C_m$ has been replaced by $C_{uo}^* - C_{um}$ and m by m_u. The relation between dC_m and C_{um} in the new integral s complex. However, C_{um} is so small compared with C_{uo}^* in these runs that it can be neglected. (C_{um} is the only 0.1 to 0.4% as large as C_{uo}^* half way through the tall column runs, and only 1 to 3% as large at the finish). With this simplification the integrals reduce to

$$e^{-N_{oL}} - 1 = -\frac{VRTC_{mf}}{NvP_o\theta_f} \qquad (16)$$

Values of N_{OL} from Equation (16) are substituted into Equation (11) along with m_u instead of m in order to find k_L.

The experimental chlorine absorption data were worked up by both of the above methods. In most cases two tall and two short column runs had been made at each new set of conditions. The sets of data were averaged and used in calculating the N_{OL}'s and k_L's.

Tabulation of the pertinent experimental and calculated results are available.†

End Effects

End effects in the oxygen absorption runs were very small as indicated by the fact that the final oxygen concentrations were almost identical in corresponding tall and short column runs. This was not true for carbon dioxide and for chlorine, where end effects were very evident. In many cases the N_{OL} for the 8 cm. depth of water was greater than the ΔN_{OL} for the incremental 22 cm. of water.

As a cross check on the validity of correcting for end effects by Equation (11), a number of runs were made with carbon dioxide and chlorine at an intermediate water depth of 19 cm. in addition to the regular depths of 8 and 30 cm. The results are plotted in Figure 3 as N_{OL} vs. depth which should be nearly proportional to the time of rise. The points are close enough to being linear to indicate that ΔN_{OL} beyond 8 cm. is substantially proportional to Δt_{t-s} as required by Equation (11).

There may be some question as to whether the paraffin oil layer may not have actually contributed to the end effect in the chlorine runs. However, omitting the oil in a control series of carbon dioxide runs increased the N_{OL} at all three depths by an appreciable and fairly uniform amount. This is also shown in Figure 3.

PREDICTED MASS TRANSFER COEFFICIENTS

The experimental liquid film mass transfer coefficients have been compared with the values predicted by Higbie's equation [Equation (2)].

The diffusivities for oxygen, carbon dioxide, and total chlorine were taken from Wilke's compilation of experimental values (*31*) corrected as necessary to 25°C. by the absolute temperature over the viscosity. The values were 2.6 × 10^{-5}, 2.07 × 10^{-5}, and 2.02 × 10^{-5} sq. cm./sec., respectively. The last figure represents a mean diffusivity for free and combined chlorine diffusing from a concentration of 10 × 10^{-5} moles to chlorine per ml. into pure water. The diffusivity for free chlorine was estimated from Wilke's correlation at 1.63 × 10^{-5} sq. cm./sec. at 25°C.

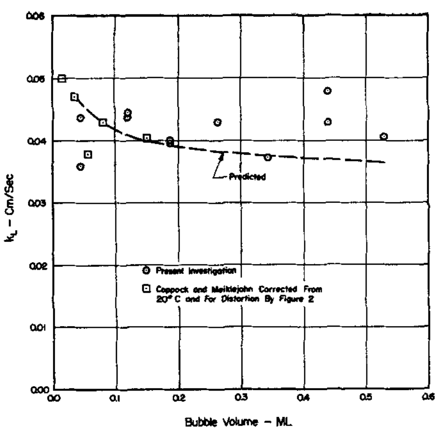

Fig. 4. Mass transfer coefficients for absorption from oxygen bubbles by water at 25°C.

The effective lives of the transient films moving over the bubble surfaces have been estimated as the times for the bubbles to rise distances equal to their own minor axes relative to the water surrounding the bubbles. For this purpose the apparent velocity of rise relative to the glass wall has been replaced by the terminal velocity of rise at very low bubbling rates in large diameter columns. The difference is assumed to be the upward velocity of the water surrounding the bubbles. The terminal velocity data used here are those of Uno Kintner (*23*). The minor axes were computed from b/r_s in Figure 2.

The predicted and observed absorption coefficients are compared in Figures 4, 5, and 6. The points for oxygen, carbon dioxide, and free chlorine are of the same order of magnitude as the theoretical predictions. They average 10 to 20% higher. The oxygen points in Figure 4 scatter more than the other two sets. This may be due to each oxygen point representing the difference between only two experimental runs, one with a tall column and one with a short column. A horizontal line at $k_L = 0.040$ gives a better empirical correlation of the data than the predicted line but has no theoretical basis. Similar oxygen data from Coppock and Meiklejohn (*3*) corrected for temperature and for bubble distortion by means of Figure 2 show better agreement with the predicted curve. The carbon dioxide points in Figure 5 and the free chlorine points in Figure 6 are more consistent. This may be due to more accurate analytical methods or to their representing the differences between averages of two or more runs. The resemblance to the predicted lines is striking. Deviations from the predicted curves are greatest for bubble volumes below 0.1 ml. Both the predicted and observed values for these smaller sizes depend on the extrapolated portion of the axes ratio curve of Figure 2. Lower values of b/b_1 in this region would reduce the deviations.

The mass transfer coefficients found in this investigation are higher than reported by Hammerton and Garner (*13*). They are about 25% higher even after correcting for differences in temperature by the square root of the diffusivities. Correcting Hammerton and Garner's data for bubble distortion would increase the spread to 30 or 35%. The techniques used were quite different, and each may have its own systematic errors. The present investigation used a maximum absorption depth of 30 cm. and attempted to reduce and correct for any end effects. Figure 2 shows

---

† Tabular material has been deposited as document 8307 with the American Documentation Institute, Photoduplication Service, Library of Congress, Washington 25, D. C., and may be obtained for $1.25 for photoprints or $1.25 for 35-mm. microfilm.

that these efforts were largely successful, but tests with still taller columns might have shown that end effects had not been completely corrected. Hammerton and Garner's results were based on volume changes of bubbles rising through the center 56 cm. of a column. The number of bubbles used was very low, since only one bubble was permitted in the column at a time. Desorption of inert gases from the water into the bubbles would have reduced both the apparent and actual absorption (*8*), although the authors were unable to detect any such effect. It seems likely that most of the differences in results are real. They may be due to more rapid or violent oscillation of the bubbles in the streams of bubbles used in the present investigation. This is substantiated to some extent by the data of Coppock and Meiklejohn (*3*) for a rapid stream of oxygen bubbles in water as indicated in Figure 4.

Baird (*1*) studied absorption from a stream of carbon dioxide bubbles, which reduces the actual slip velocity and results in absorption coefficients higher than those predicted from the terminal velocity. However, no significant deviation from the theoretical absorption rate was observed for bubble diameters less than about 1 cm., whereas the carbon dioxide bubbles in the present experiments had diameters ranging from 0.41 to 0.92 cm.

The predicted and observed chlorine absorption coefficients based on total chlorine concentrations are compared with those for carbon dioxide in Figure 5. The predicted curves are almost identical, but the observed total chlorine values are only a fourth as large as the carbon dioxide values. This is in line with Vivian and Whitney's results for absorption of chlorine in water in packed columns. It proves that the reaction between chlorine and water must be a long way from chemical equilibrium within the transient films.

The similarity between the free chlorine and carbon dioxide coefficients in relation to their respective predicted curves in Figures 5 and 6 suggests that the amount of chlorine hydrolysis in the transient films is small. Spalding (*22*) has shown that chlorine reacts with both water and hydroxyl ions, the rate controlling reaction being dependent on the pH of the absorbing liquid. At pH values between 3 and 10.5, Equation (17) is the controlling mechanism:

$$Cl_2 + H_2O \rightleftharpoons H^+ + Cl^- + HOCl \qquad (17)$$

For short reaction times in this pH range the forward reaction predominates, thus making applicable Danckwerts' solution for unsteady state diffusion accompanied by a first-order irreversible reaction (*6*).

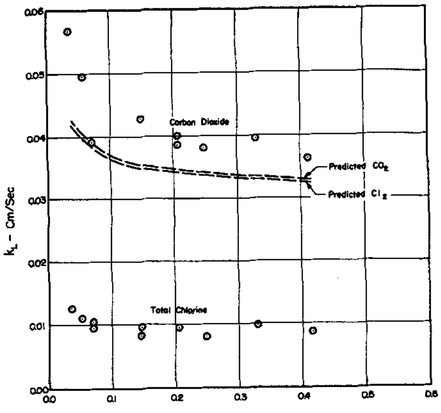

Fig. 5. Mass transfer coefficients for absorption from carbon dioxide-air and from chlorine-air bubbles by water at 25°C.

Danckwerts' solution can be expressed as a correction factor for Higbie's predicted k_L as follows:

$$k_L = 2\sqrt{D/\pi\, t_e} \cdot \Phi(\beta) \qquad (18)$$

where

$$\Phi(\beta) = \left(\sqrt{\beta} + \frac{1}{2\sqrt{\beta}}\right) \cdot \int^{\sqrt{\beta}} e^{-y^2}\, dy + \frac{1}{2} e^{-\beta} \qquad (19)$$

and where $\beta = k_r t_e$. Equation (19) can be solved by means of error function tables or by its series expansion:

$$\Phi(\beta) = 1 + \frac{\beta}{3} - \frac{\beta^2}{30} - \frac{\beta^3}{210} - \ldots + \frac{(-1)^{n+1}\beta^n}{n!(2n-1)(2n+1)} + \ldots \qquad (20)$$

Equation (20) has been derived independently by series integration of the original partial differential equations. For values of β of 2 or higher the following approximation is simple and quite accurate:

$$\Phi(\beta) = \frac{\sqrt{\pi}}{2}\left(\sqrt{\beta} + \frac{1}{2\sqrt{\beta}}\right) \qquad (21)$$

Several differing values of the pseudo first-order reaction rate constant k_r for the hydrolysis of chlorine are given in the literature. Brian, Vivian, and Habib (*2*) arrived at a value of 13.7 sec.$^{-1}$ at 25°C. using a short wetted column. Spalding (*22*) used a laminar liquid jet and obtained a k_r of 20.9 for the mid pH range. These two values give $\Phi(\beta)$'s ranging from 1.07 to 1.11 and 1.10 to 1.16, respectively, corresponding to the range of t_e's in the present experiments. The resulting curves for the corrected k_L's for both cases are included on Figure 6.

The predicted values of k_L assuming a reaction rate constant of 13.7, are in good agreement with the observed results except at very low bubble volumes. This value of the rate constant also compares more favorably with previous measurements by Lifshitz and Perlmutter-Haymen (*19*) and by Solodushenkov and Shilov (*21*).

The predicted k_L's could be a little high if the diffusivity of free chlorine is less than that given by Wilke's correlation. In this connection Vivian and Peaceman (*25*) have reported a value of 1.46 × 10^{-5} sq. cm./sec. for free chlorine in hydrochloric acid solution. This value would have lowered the predicted k_L's about 5%.

SUMMARY

The use of Higbie's equation for unsteady state diffusion from gas bubbles has been reviewed. It is pointed out that a ringlike element of interface could pass completely over the entire surface of a spherical bubble without change in area under certain conditions.

Absorptions from streams of bubbles of various size in a column of water have been determined under batch-by-batch conditions with pure oxygen, 10% carbon dioxide in air, and 10% chlorine in air. Equations have been developed for computing the mass transfer coefficients from the batch-by-batch data. Corrections have been applied for increased bubble area due to bubble distortion. The observed coefficients have been compared with those predicted from Higbie's equation for a transient film life equal to the time for the bubble to rise through its minor axis relative to the surrounding liquid.

The observed coefficients for oxygen and carbon dioxide absorption average 10 to 20% higher than the predictions. They agree with similar oxygen data of Coppock and Meiklejohn but are appreciably higher than the coefficients found by Hammerton and Garner using only one bubble in the column at a time.

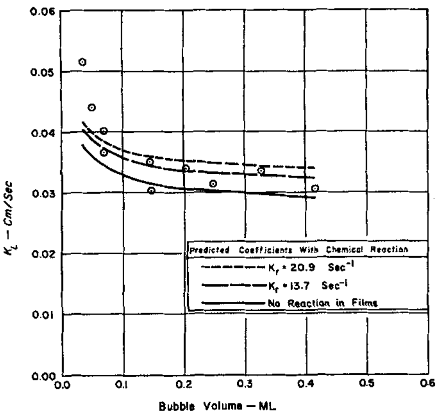

Fig. 6. Mass transfer coefficients based on free chlorine concentrations for absorption from chlorine-air by water at 25°C.

The observed coefficients for chlorine absorption based on total chlorine concentrations are only a fourth as great as for carbon dioxide of nearly the same diffusivity. Much better agreement with predictions is obtained if the coefficients are based on free chlorine concentrations on the assumption of negligible chemical reaction with water within the transient films. Good agreement with predictions is obtained, however, if the coefficients are based on the absorption of free chlorine with simultaneous irreversible chemical reaction with the water in the transient film. A pseudo first-order reaction rate constant of 13.7 sec.$^{-1}$ gives good agreement with the observed absorption coefficients.

It appears that Higbie's equation, or equations much like it, must be an essential part of any analysis or method of predicting mass transfer data from bubbles.

NOTATION

a = area per gas bubble, sq.cm.
a_s = area of sphere of same volume as bubble, sq.cm.
b = half minor axis of oblate spheroid, cm.
b_1 = half major axis of oblate spheroid, cm.
C = solute concentration, g.-moles/ml.
C^* = equilibrium concentration, g.-moles/ml.
C_m = main body concentration, g.-moles/ml.
D = diffusivity, sq.cm./sec.
E = eccentricity, Equation (5)
h = vertical distance from equator of sphere to differential circular zone
k = mass transfer coefficient, cm./sec.
k_1 and k_2 = forward and reverse chemical reaction rate constants
k_L = liquid-phase mass transfer coefficient, cm./sec.
k_r = first-order chemical reaction rate constant, sec.$^{-1}$
k_w = ion product of water
m = slope of $p - C$ plot, (mm.)Hg/(g.-moles/ml.)
N = bubbling rate, bubbles/sec.
n = solute gas transferred per bubble, g.-moles
N_{OL} = defined by Equation (12)
ΔN_{OL} = $N_{OLt} - N_{OLs}$
P = partial pressure of solute gas, mm. Hg
r_s = radius of sphere of same volume as bubble, cm.
R = gas constant
t = absorption or reaction time for one bubble, sec.
T = temperature, °K.
t_e = life of transient film, sec.
Δt_{t-s} = difference between absorption times in tall and short columns, sec.
V = volume of the liquid in the column, ml.
v = volume of each gas bubble, ml.
U_t' = terminal velocity of gas bubbles, cm./sec.
U_t = velocity of gas bubbles relative to column wall, cm./sec.

Greek Letters

α = angle between pole of sphere and radii to differential circular zone
β = $k_r t_e$, dimensionless
θ = time during absorption run, sec.
$\Phi(\beta)$ = correction factor defined by Equation (19)

Subscripts

f = at finish of run
i = at the interface
o = at zero time or bottom of column
p = at top of column
s and t = short and tall columns, respectively
u = free or unreacted chlorine

LITERATURE CITED

1. Baird, M. H. I., and J. F. Davidson, *Chem. Eng. Sci.*, **17**, 87 (1962).
2. Brian, P. L. T., J. E. Vivian, and A. G. Habib, *A.I.Ch.E. Journal*, **8**, 205 (1962).
3. Coppock, P. D., and G. T. Meiklejohn, *Trans. Inst. Chem. Engrs. (London)*, **29**, 75 (1951).
4. Coulson, J. M., and S. J. Skinner, *Chem. Eng. Sci.*, **1**, 197-211 (1952).
5. Danckwerts, P. V., *Research*, **2**, 494 (1949).
6. ———, *Trans. Faraday Soc.*, **46**, 300 (1950).
7. ———, *Ind. Eng. Chem.*, **43**, 1460-1467 (1951).
8. Datta, R., D. Napier, and D. M. Hewitt, *Trans. Inst. Chem. Engrs. (London)*, **28**, 14-26 (1950).
9. Gaillard, D. P., *Ind. Eng. Chem.*, **11**, 745-747 (1919).
10. Garner, F. H., and A. H. P. Skelland, *Trans. Inst. Chem. Engrs. (London)*, **29**, 315 (1951).
11. ———————, *Ind. Eng. Chem.*, **46**, 1255 (1954).
12. Geddes, R. L., *Trans. Am. Inst. Chem. Engrs.*, **42**, 79-105 (1946).
13. Hammerton, D., and F. H. Garner, *Trans. Inst. Chem. Engrs. (London)*, **32**, S18-S24 (1954).
14. Hodgman, C. D., ed., "Handbook of Chemistry and Physics," 23 ed., p. 296, Chemical Rubber Publishing Co., Cleveland, Ohio (1939).
15. Higbie, R. W., *Trans. Am. Inst. Chem. Engrs.*, **31**, 365-89 (1935).
16. Hughes, R. R., and E. G. Gilliland, *Chem. Eng. Progr.*, **48**, 497-504 (1952).
17. "International Critical Tables," Vol. 3, pp. 257-260, McGraw-Hill, New York (1928).
18. Li, P. S., Ph.D. thesis, Univ. of Washington, Seattle, Washington (1953).
19. Lifshitz, A., and B. Perlmutter-Haymen, *J. Phys. Chem.*, **64**, 1663 (1960).
20. Sherwood, T. K., J. E. Evans, and J. V. A. Longcor, *Ind. Eng. Chem.*, **31**, 1144-50 (1939).
21. Solodushenkov, S. N., and E. A. Shilov, *J. Phys. Chem. (USSR)*, **19**, 405 (1945).
22. Spalding, C. W., *A.I.Ch.E. Journal*, **8**, 685 (1962).
23. Uno, Seiji, and R. C. Kintner, *ibid.*, **2**, 420 (1956).
24. Van Krevelen, D. W., and P. J. Hoftjzer, *Chem. Eng. Progr.*, **46**, 29-35 (1950).
25. Vivian, J. E., and D. W. Peaceman, *A.I.Ch.E. Journal*, **2**, 437 (1956).
26. ———, and R. P. Whitney, *Chem. Eng. Progr.*, **43**, 691-702 (1947).
27. West, F. B., P. A. Robinson, A. C. Morgenthaler, Jr., T. R. Beck, and D. K. Mcgregor, *Ind. Eng. Chem.*, **43**, 234 (1951).
28. ———, A. J. Herrman, A. T. Chong, and L. E. K. Thomas, *ibid.*, **44**, 625-31 (1952).
29. ———, W. D. Gilbert, and T. Shimizu, *ibid.*, pp. 2470-8.
30. Whitney, R. P., and J. E. Vivian, *ibid.*, **33**, 741-4 (1941).
31. Wilke, C. R., *Chem. Eng. Progr.*, **45**, 218-24 (1949).

Manuscript received February 24, 1964; revision received January 12, 1965; paper accepted January 15, 1965.